PROGRESS IN PHOTOVOLTAICS: RESEARCH AND APPLICATIONS
Prog. Photovolt: Res. Appl. (2012)
Published online in Wiley Online Library (wileyonlinelibrary.com). DOI: 10.1002/pip.2244

ACCELERATED PUBLICATION

Wide bandgap Cu(In,Ga)Se_2 solar cells with improved energy conversion efficiency

Miguel A. Contreras[1]*, Lorelle M. Mansfield[1], Brian Egaas[1], Jian Li[1], Manuel Romero[1], Rommel Noufi[1], Eveline Rudiger-Voigt[2] and Wolfgang Mannstadt[2]

[1] National Renewable Energy Laboratory, Golden, CO, USA
[2] Schott AG, Mainz, Germany

ABSTRACT

We report on improvements to the energy conversion efficiency of wide bandgap ($E_g > 1.2$ eV) solar cells on the basis of $CuIn_{1-x}Ga_xSe_2$. Historically, attaining high efficiency (>16%) from these types of compound semiconductor thin films has been difficult. Nevertheless, by using (a) the alkaline-containing high-temperature EtaMax glass substrates from Schott AG, (b) elevated substrate temperatures of 600–650 °C, and (c) high vacuum evaporation from elemental sources following National Renewable Energy Laboratory's three-stage process, we have been able to improve the performance of wider bandgap solar cells with $1.2 < E_g < 1.45$ eV. The current density–voltage (J–V) data we present includes efficiencies >18% for absorber bandgaps of ~1.30 eV and efficiencies of ~16% for bandgaps up to ~1.45 eV. In comparing J–V parameters in similar materials, we establish gains in the open-circuit voltage and, to a lesser degree, the fill factor value, as the reason for the improved performance. The higher voltages seen in these wide gap materials grown at high substrate temperatures are due to reduced recombination. We establish the existence of random and discrete grains within the CIGS absorbers that yield limited or no generation/collection of minority carriers. We also show that interfacial recombination is the main mechanism limiting additional enhancements to open-circuit voltage and therefore performance. Solar cell results, absorber materials characterization, and experimental details and discussion are presented. Copyright © 2012 John Wiley & Sons, Ltd.

KEYWORDS

CIGS; wide gap; chalcogenides; high efficiency; thin film; high temperature

***Correspondence**

Miguel Contreras, National Renewable Energy Laboratory, Golden, CO, USA.
E-mail: Miguel.contreras@nrel.gov

Received 10 January 2012; Revised 28 February 2012; Accepted 20 April 2012

1. INTRODUCTION

$CuIn_{1-x}Ga_xSe_2$ (CIGS)-based solar cells have achieved the highest energy conversion efficiency (>20%) among photovoltaic (PV) thin-film materials. These solar cells are typically made from CIGS alloys with low Ga content ($x \sim 0.3$), resulting in absorbers with a direct energy bandgap value of ~1.1–1.2 eV. It is desirable to develop wider bandgap absorbers for reasons such as (i) tuning E_g to 1.4 eV, as suggested by the theoretical calculations for optimum conversion efficiency; (b) improving the performance of PV cells under real working/operating conditions; and (c) developing multi-junction thin-film polycrystalline solar cells that attain even higher energy conversion efficiency than today's state of the art in single-junction cells.

In practice, low E_g single-junction solar cells suffer from a great loss of power output when their operating temperature exceeds 25 °C. This is referred to as the Maximum Power Thermal Coefficient (MPTC), which is defined as the percentage change in power output per degree Celsius and is typically quoted in the nameplate of commercial modules. Crystalline silicon ($E_g \sim 1.1$ eV), for example, has a −0.50%/°C MPTC, which is a little worse than CIGS at −0.44%/°C ($E_g \sim 1.2$ eV). On the other hand, other thin-film PV technologies such as a-Si and CdTe ($E_g \sim 1.45$ eV) show MPTCs of −0.17%/°C and −0.25%/°C, respectively. Because modules under real operating conditions can reach temperatures as high as 50–75 °C depending on location and, evidently, time of year, the efficiency (or power output) of low bandgap cells and modules are effectively derated by at least 11% and, in some instances, as much as 25%.

It is also desirable to fabricate solar cells and modules that produce higher output voltages and a lower current (as wider gap solar cells should) to minimize the intrinsic resistive losses ($R*I^2$) in a module or cell. Historically, the high-efficiency regime for CIGS has been limited to the low E_g materials, and efficiencies attained for CIGS materials with $E_g > 1.2$ eV have been consistently low [1,2]. In this contribution, we report on improvements to CIGS materials with $E_g > 1.2$ eV and discuss the solar cell parameters, processes, and some material physical properties that have enabled high efficiency (>16%) for E_g values (so far) up to ~1.45 eV.

2. EXPERIMENTAL

The substrates we have used in this experimentation are the EtaMax specialty high-temperature alkaline-containing glasses developed by Schott AG. These specialty substrates allow processing temperatures above those enabled by traditional soda-lime silicate glass (SLG)—typically, <550 °C—and they can withstand processing temperatures up to 670 °C without deformation. In addition to withstanding high temperatures, the glass has an adapted coefficient of thermal expansion matched for the CIGS process and a tailored Na release at elevated temperatures, both important features for high-efficiency CIGS solar cells. We also used evaporation from elemental sources and applied the patented National Renewable Energy Laboratory (NREL) three-stage process [3,4] for the fabrication of the absorbers and selected substrate temperatures in the range of 600–650 °C.

All solar cells fabricated for this study have a standard ZnO/CdS/CIGS/Mo layered structure where the Mo back contact of the solar cells is deposited by direct current sputtering, the CdS by chemical bath deposition, and the ZnO by radio frequency sputtering from ceramic targets. These lab-scale (area, ~0.42 cm^2) solar cells also incorporate a top contact grid with ~5% obscuration loss made of nickel and aluminum and deposited by electron beam evaporation. Selected champion solar cells were coated with an antireflection layer of MgF_2.

3. SOLAR CELL RESULTS

The best solar cells (champion cells) fabricated in this work were submitted for current density–voltage (*J–V*) certification, and a summary of those efficiency results (versus bandgap) are shown in Figure 1. All relevant *J–V* parameters for cells in Figure 1 are shown in Table I. The energy bandgap values for the data in Figure 1 (and Table I) were determined from certified quantum efficiency (QE) curves by arbitrarily assigning an "effective" bandgap value to the energy calculated from the wavelength value where a 20% QE value is observed for the long wavelengths. This approach and methodology for estimating an "effective" bandgap value in CIGS solar cells has been described in [5] where we reported some preliminary results in wide bandgap CIGS solar cells.

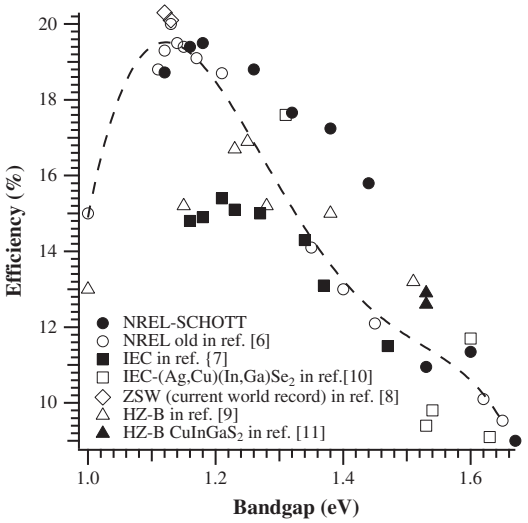

Figure 1. Solar cell efficiency versus $CuIn_{1-x}Ga_xSe_2$ absorber bandgap value.

Table I. *J–V* parameters of wide gap $CuIn_{1-x}Ga_xSe_2$ solar cells.

E_g (eV)	Efficiency (%)	V_{oc} (V)	FF (%)	J_{sc} (mA/cm^2)
1.12	18.7	0.711	78.62	33.5
1.16	19.4	0.765	78.99	32.1
1.18	19.5	0.759	78.8	32.6
1.26	18.8	0.801	80.70	29.1
1.32	17.7	0.801	77.21	28.5
1.38	17.2	0.817	76.65	27.5
1.44	15.8	0.813	72.17	26.9
1.53	11.0	0.829	65.32	20.2
1.60	11.4	0.766	71.02	20.9
1.67	9.0	0.795	69.22	16.4

FF, fill factor.

From the data shown in Figure 1, we are able to report a significant improvement to the efficiency of wide gap CIGS solar cells for 1.2 eV < E_g < 1.45 eV. Figure 1 shows for comparison purposes the efficiency values published in the literature for other related works (including our own) in this area of wide gap chalcogenides [6–11].

From the *J–V* parameters obtained, we can attribute the enhancement in performance for CIGS solar cells with 1.20 eV < E_g < 1.45 eV to higher open-circuit voltage (V_{oc}) values as compared with previous results, as shown in the graph of V_{oc} versus E_g in Figure 2. The data in Figure 2 show not just the higher absolute values for the voltage but also

(i) the breakdown of the expected linear behavior of V_{oc} as a function of E_g for solar cells with $E_g > 1.35$ eV and
(ii) a saturation of the V_{oc} values at ~830 mV for solar cells with $E_g > 1.35$ eV.

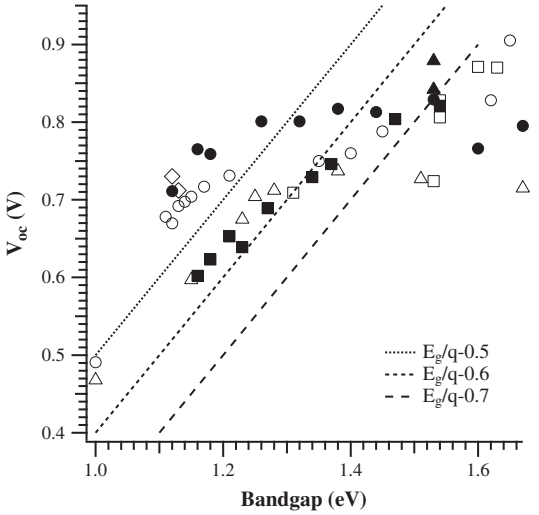

Figure 2. V_{oc} versus $CuIn_{1-x}Ga_xSe_2$ absorber bandgap value. Data symbols as noted in Figure 1.

The fill factor (FF) values and their trend with increased E_g (or Ga content) for the wide gap CIGS solar cells reported here are no different than those values seen in CIGS grown in SLG. The maximum FF values (77–80%) are attained for cells with $1.20\,eV < E_g < 1.35\,eV$, and for higher energy gap values, the FF values decrease gradually to values of ~70% for $E_g \sim 1.67\,eV$ (or $x = 1.0$) in the pure $CuGaSe_2$ case.

Similarly to the FF data, the short-circuit current density (J_{sc}) values of the high-temperature CIGS solar cells do not differ from what has been seen and reported for CIGS absorber materials grown on SLG; our experimental J_{sc} values follow the expected linear behavior of decreasing J_{sc} values with increased bandgap (or Ga content).

4. SOLAR CELL AND ABSORBER ANALYSIS

We previously reported in [5] that the higher V_{oc} values observed are due to a decrease in the value of the dark saturation current density (J_o) on the basis of experimental and comparative measurements of such parameters. We also determined in that preliminary work that grain boundary optoelectronic activity in these wide gap CIGS solar cells shows a similar behavior to that observed in high-efficiency CIGS cells. Specifically, we have reported from cathode luminescence (CL) analysis of high-efficiency CIGS absorbers [12] a phenomenon we have referred to as a "red shift" in the CL energy emission from grain boundary (GB) regions; we observe a small yet measurable shift in the donor to acceptor luminescence emission peak energy from GB regions toward lower energy values as compared with the emission from grain interiors (GI). This "red shift" is characteristic of high-efficiency CIGS materials. The wide bandgap CIGS materials we report in this contribution do show this "red shift" behavior in GB areas, and therefore, we attribute part of the enhanced performance of these wide gap CIGS solar cells to the improvement in GB optoelectronic activity. Figure 3 shows CL data for selected wide gap CIGS materials to exemplify the GB (and GI) activity discussed here. For additional information, a color-coded mapping of such CL emission has been presented in [5].

Nonetheless, the wide gap CIGS cells still suffer from a significant interfacial recombination as established from our temperature-dependent *J–V* measurements shown in Figure 4; the extrapolation to $T = 0K$ for the V_{oc} values indicate that the wide gap cells do not extrapolate to their expected bandgap value and extrapolate only to $qV_{oc} \sim 1.2\,eV$. Also, in [5], we indicate a decline in QE as the Ga content is increased in the CIGS absorbers; the overall collection efficiency, particularly for the long wavelengths, falls in value and leads to lower J_{sc} values than what could be expected for a given bandgap value.

By using a combination of scanning electron microscopy (SEM) and an electron beam-induced current (EBIC) technique performed in the same areas as the SEM micrographs, we have been able to take a more detailed look at the carrier generation/collection in these types of solar cells (Figures 5–8). From these EBIC data, it is clear that the effective collection depth deteriorates as the Ga content is increased, and the lower QE values measured in cells with increased Ga content are consistent with the reduced

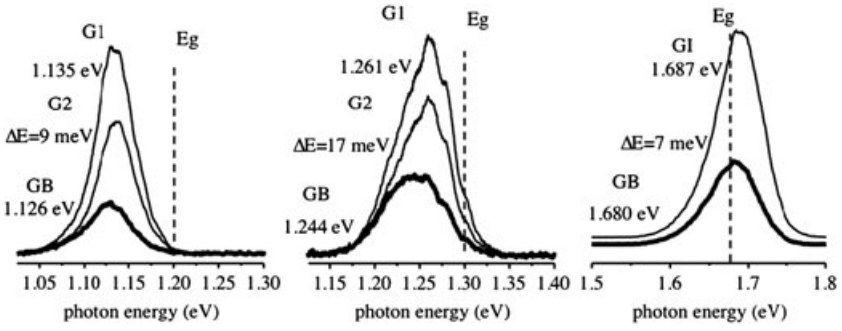

Figure 3. Cathode luminescence optical emission from grain interior (GI, G1, G2) and grain boundary (GB) areas for $CuIn_{1-x}Ga_xSe_2$ absorbers with bandgaps of ~1.2 eV (left), 1.3 eV (middle), and 1.67 eV (right). ΔE denotes the difference in peak energy emission between GI and GB.

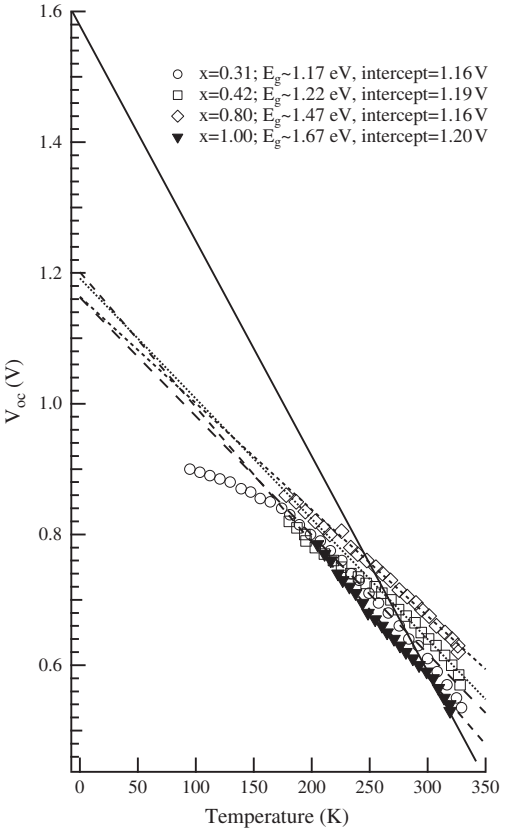

Figure 4. $V_{oc}(T)$ for selected wide bandgap $CuIn_{1-x}Ga_xSe_2$ solar cells.

effective collection shown in the EBIC maps. There are also some interesting features in the EBIC maps reported here, features that were unexpected and rather surprising; some grains show total loss of collection, as indicated by the black colored grains in Figures 5–8, and/or there is an abrupt loss of collection in some cases where a grain with high collection efficiency resides right next to another with poorer or no collection at all. Such "dead" grains, for lack of a better word, seem to be randomly located within the bulk of the thin-film absorbers, and it is unclear at this time if that loss of collection is due to the grains themselves or due to the interfaces between them. More work is necessary to determine the actual cause of these phenomena.

5. DISCUSSION

From [5] and considering standard one-dimensional solar cell equations, we have established that the higher voltages seen in the high-temperature CIGS solar cells arise from a reduced reverse saturation current density value and not from an increase in carrier concentration. Additionally, the fact that GB CL emissions in the wide gap CIGS materials reported here show a "red shift" relative to the GI suggests to us that the grain boundaries now present optoelectronic properties that aid in reducing recombination in such areas. It is therefore clear to us that the GB activity in high-temperature CIGS absorber materials has been improved and now matches or resembles the behavior seen in standard high-efficiency solar cells. We point out this CL GB phenomenon had not been observed in previous wide gap materials that were grown at lower substrate temperature. The true nature (either chemical or structural) of these *beneficial* defects at grain boundaries may still be a matter of discussion, but whatever their nature is, we are inclined to think they are the main reason for the improvements to wider gap CIGS solar cells reported here.

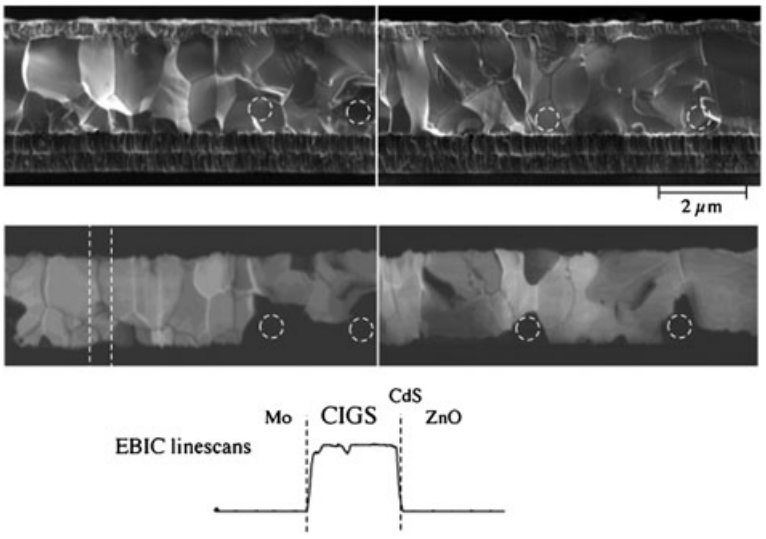

Figure 5. Scanning electron microscopy (top), electron beam-induced current (EBIC) map (middle), and EBIC linescans (bottom) for standard high-efficiency $CuIn_{1-x}Ga_xSe_2$ (CIGS) with $E_g \sim 1.16$ eV.

DOI: 10.1002/pip

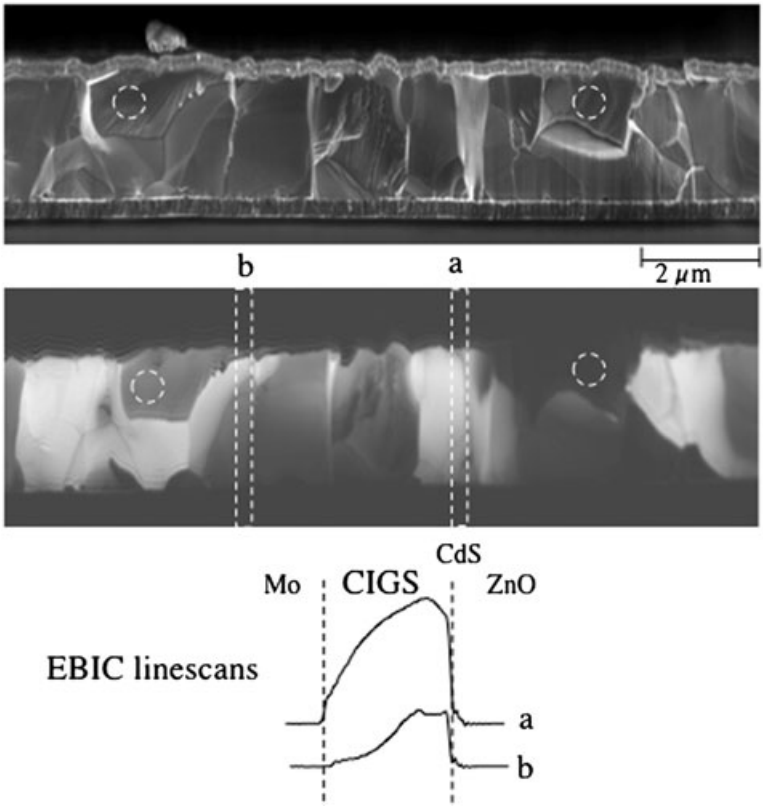

Figure 6. Scanning electron microscopy (top), electron beam-induced current (EBIC) map (middle), and EBIC linescans (bottom) for $CuIn_{1-x}Ga_xSe_2$ (CIGS) with $E_g \sim 1.2$ eV.

The J–$V(T)$ data obtained suggest that an important limitation for higher efficiency values in wide gap CIGS solar cells is interfacial recombination. We remark that a close examination of the $V_{oc}(T)$ data in Figure 4 for wide gap CIGS reveals that the curves are not, strictly speaking, linear in nature within the temperature range studied, and, in a simple linear curve-fitting routine for $175\text{K} < \text{T} < 325\text{K}$, they do not extrapolate at $T = 0$K to the $qV_{oc} \sim E_g$ of the absorber material except for the lower bandgap materials ($E_g < 1.2$ eV). Indeed, some of the experimental curves developed show different slopes for different temperature ranges, similar to (but less pronounced than) the behavior observed for the $x = 0.31$ case for $T < 175$K in Figure 4. In particular, for the case where $x = 1$, the $V_{oc}(T)$ experimental data has a higher slope value for $280\text{K} < T < 325\text{K}$, which in this case and for that (limited) temperature range would extrapolate at $T = 0$K to $qV_{oc} \sim 1.6$ eV (illustrated by the solid line in Figure 4), roughly corresponding to the bandgap value for $CuGaSe_2$ (CGS). However, when considering temperatures less than 280K, the slope of the $V_{oc}(T)$ for CGS no longer extrapolates to that value. This is in agreement with previously reported observations in CGS solar cells made by Young *et al*. in [13] where a similar nonlinear behavior of $V_{oc}(T)$ is reported for such solar cells.

On a separate characterization topic, the EBIC maps indicate some strong recombination in discrete and apparently random grains and/or grain interfaces where carrier collection is significantly reduced or in some cases, completely lost. This is an intriguing finding that will evidently need further clarification, particularly as to the root cause of these phenomena: is this due to some bulk property of the grain interior? Or is it related to the surface and the nature of the interface between those grains, that is, is it a structural argument similar to that discussed by Abou-Ras *et al*. in [14], or could it be chemical in nature (microdomains of α and β CIGS phases, impurities, or other)? Stanberry *et al*. have proposed that the α and β phases may segregate spontaneously to form an interpenetrating three-dimensional network of charge-separating junctions that give rise to the operative mode of current collection in CIGS solar cells [15]. There is also the theoretical work of Metzger [16] where such networks are modeled under the assumption of no interface recombination between domains (recombination assumed to be zero). The key findings in [16] indicate that modeled J_{sc} values are strongly dependent on domain size, and in particular, J_{sc} values are significantly affected when domain sizes are either very small (<0.04 μm) or rather large (>0.3 μm). Therefore, at this point, we cannot ignore the possibility that the observed features in the EBIC maps

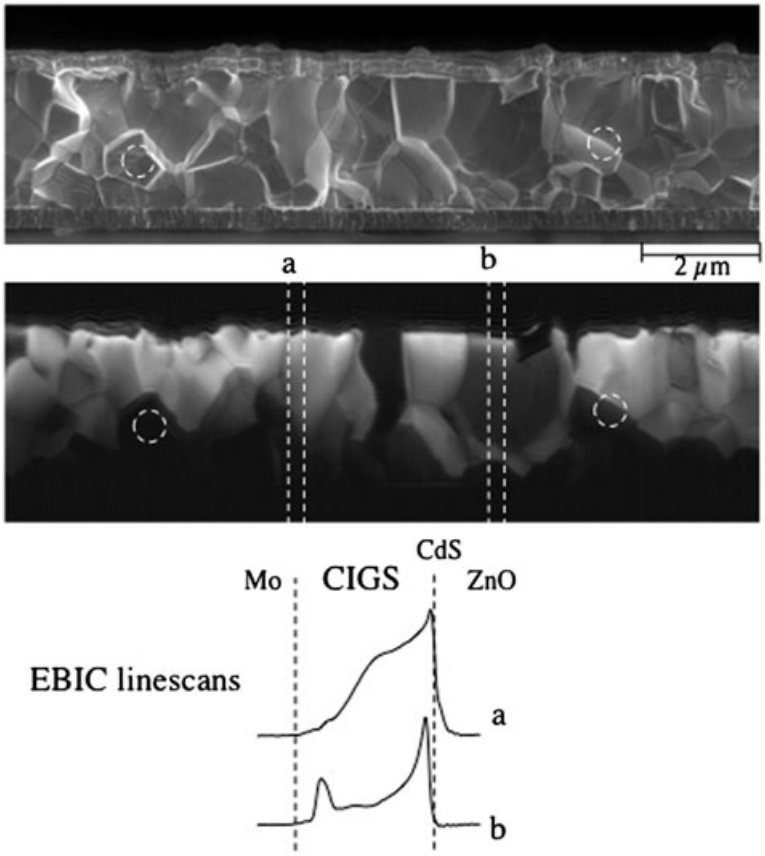

Figure 7. Scanning electron microscopy (top), electron beam-induced current (EBIC) map (middle), and EBIC linescans (bottom) for $CuIn_{1-x}Ga_xSe_2$ (CIGS) with $E_g \sim 1.4$ eV.

may be related to microdomains of α and β CIGS phases interacting with each other.

It is likely that other limiting factors are present (aside from the grain boundary, interfacial recombination, and microdomains) that limit the V_{oc} and the performance of the widest gap materials ($E_g > 1.45$ eV). We speculate that factors such as band alignment between the CdS and the wider gap CIGS materials may not be optimum, and perhaps, alternatives to CdS such as wider gap "buffer" layers may be needed to discern more limiting factors for solar cells made from absorbers with $E_g > 1.5$ eV. There could be other reasons as well, such as the nature of the electrical conductivity type at the usually Cu-depleted surface region of these materials. Naturally, more investigations are necessary in all these areas, but within the scope of this work, we can already see and report significant improvements to the performance of wide gap CIGS solar cells.

6. CONCLUSIONS

We have experimented with higher-than-standard substrate temperatures for the growth of CIGS materials with $0.3 < x < 1.0$. The use of higher processing temperatures (600–650 °C) than the standard 550–600 °C typically used have led to significant improvements in the energy conversion efficiency of wide gap CIGS solar cells with bandgaps up to 1.45 eV. The main parameter that has improved is the output voltage of the cells as compared with previous CIGS materials grown on SLG substrates. A reduction in the reverse saturation current density value is responsible for the enhanced voltages attained. The high-temperature CIGS materials grown also show improvements to their grain boundary characteristics and now display properties similar to those found in high-efficiency CIGS materials. Although we report efficiency improvements for CIGS bandgaps in the range $1.2\text{ eV} < E_g < 1.45\text{ eV}$, the widest bandgap solar cells ($E_g > 1.5$ eV) are still limited in performance, and their efficiencies are still <15%. We have found from EBIC studies the presence of discrete and random grains and/or grain interfaces that lead to a major loss in carrier collection. Such features are not completely understood at this point, but structural and/or chemical arguments may be behind that behavior. Additional experimental and theoretical work is necessary to finally isolate and identify the most significant limiting factors in the efficiency, output current, and voltage for those solar cells.

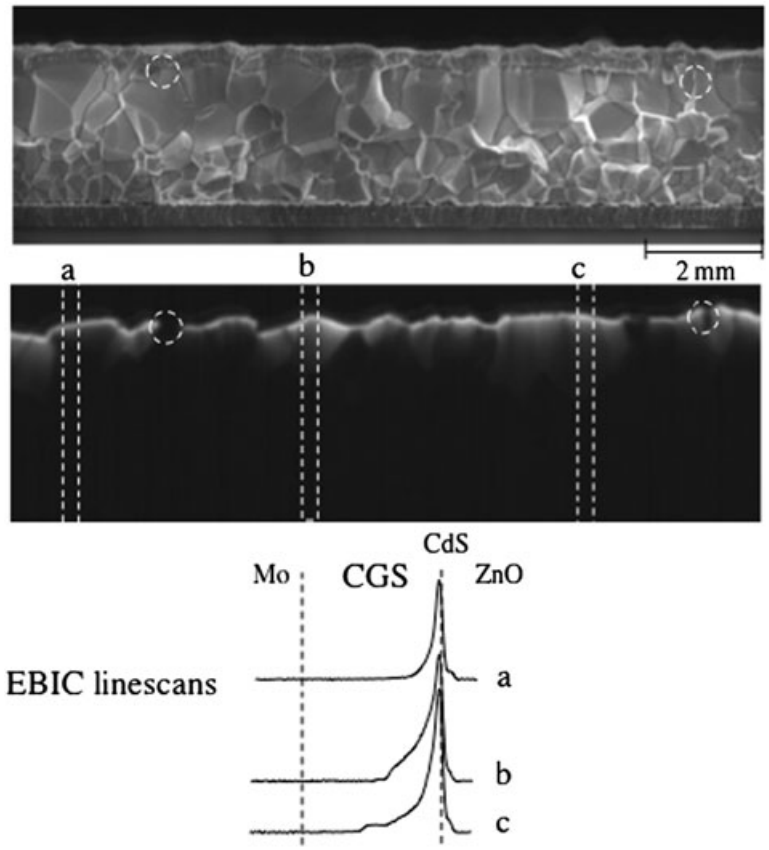

Figure 8. Scanning electron microscopy (top), electron beam-induced current (EBIC) map (middle), and EBIC linescans (bottom) for $CuIn_{1-x}Ga_xSe_2$ (CIGS) with $E_g \sim 1.67$ eV.

ACKNOWLEDGEMENTS

The authors would like to thank Clay DeHart, Marty Scott, and Carolyn Beal for their work in processing the solar cells made for this work. This work was supported by the US Department of Energy under Contract No. DE-AC36-08GO28308 with NREL.

REFERENCES

1. Herberholz R, Nadenau V, Rühle U, Köble C, Schock HW, Dimmler B. Prospects of wide-gap chalcopyrites for thin film photovoltaic modules. *Solar Energy Materials and Solar Cells* 1997; **49**: 227–237.
2. Gloeckler M, Sites JR. Efficiency limitations for wide-band-gap chalcopyrite solar cells. *Thin Solid Films* 2005; **480-481**: 241–245.
3. Contreras M, Gabor AM, Tennant A, Asher S, Tuttle J, Noufi R. 16.4% Total-area Conversion Eficiency Thin-film Polycrystalline MgF/ZnO/CdS/Cu(In,Ga)Se_2/Mo Solar Cell. *Progress in Photovoltaics* 1994; **2**: 287–292.
4. Gabor A, Truttle JR, Contreras M, Albin DS, Franz A, Niles DW, Noufi R. High-Efficiency Thin-Film Cu(In, Ga)Se2 Solar Cells: Achievement of a Confirmed World-Record 16.4% Total-Area Efficiency. *Proceedings from the 12th European Photovolaic Solar Energy Conference* (H.S. Stephens and Assoc., UK), Amsterdam, The Netherlands, 11-15 April 1994; 939-943.
5. Contreras MA, Mansfield LM, Egaas B, Li J, Romero M, Noufi R, Rudiger-Voigt E, Mannstadt W. Improved energy conversion efficiency in wide bandgap Cu(In, Ga) Se_2 solar cells. *Proceedings of the 37th IEEE Photovoltaic Specialists Conference*, 2011 (in press).
6. Contreras MA, Ramanathan K, AbuShama J, Hasoon F, Young DL, Egaas B, Noufi R. Diode Characteristics in State-of-the-Art ZnO/CdS/$CuIn_{1-x}Ga_xSe_2$ Solar Cells. *Progress in Photovoltaics: Research and Applications* 2005; **13**: 209–216.
7. Shafarman WN, Klenk R, McCandless BE. Characterization of Cu(In,Ga)Se_2 Solar Cells with High Ga Content. *Proceedings of the 25th IEEE Photovoltaic Specialists Conference*, 1996; 763.

8. Jackson P, Hariskos D, Lotter E, Paetel S, Wuerz R, Menner R, Wischmann W, Powalla M. New world record efficiency for $Cu(In,Ga)Se_2$ thin-film solar cells beyond 20%. Twenty fifth EU PVSEC, WCPEC-5, Valencia, Spain 2010.
9. Eisenbarth T, Unold T, Caballero R, Kaufmann CA, Abou-Ras D, Schock H-W. Origin of defects in $CuIn_{1-x}Ga_xSe_2$ solar cells with varied Ga content. *Thin Solid Films* 2009; **517**: 2244–2247.
10. Hanket GM, Boyle JH, Shafarman WN. Characterization and device performance of $(Ag,Cu)(In,Ga)Se_2$ absorber layers. *Proceedings of the 34th IEEE Photovoltaic Specialists Conference*, 2009; 1240.
11. Merdes S, Mainz R, Klaer J, Meeder A, Rodriguez-Alvarez H, Schock HW, Lux-Steiner MCh, Klenk R. 12.6% efficient $CdS/Cu(In,Ga)S_2$-based solar cell with an open circuit voltage of 879 mV prepared by a rapid thermal process. *Solar Energy Materials and Solar Cells* 2011; **95**: 864–869.
12. Contreras MA, Repins I, Metzger WK, Romero M, Abou-Ras D. Se activity and its effect on $Cu(In,Ga)Se_2$ photovoltaic thin films. *Physica Status Solidi A* 2009; **206**(5): 1042–1048.
13. Young DL, Keane J, Duda A, AbuShama JAM, Perkins CL, Romero M, Noufi R. Improved Performance in $ZnO/CdS/CuGaSe_2$ Thin-Film Solar Cells. *Progress in Photovoltaics: Research and Applications* 2003; **11**: 535–541.
14. Abou-Ras D, Pantleon K. The impact of twinning on the local texture of chalcopyrite-type thin films. *Physica Status Solidi* (RRL) 2007; **1**(5): 187–189.
15. Stanbery BJ. The intra-absorber junction (IAJ) model for the device physics of copper indium selenide-based photovoltaics. *Proceedings of the 31st IEEE Photovoltaic Specialists Conference* 2005; 355.
16. Metzger WK. The potential and device physics of interdigitated thin-film solar cells. *Journal of Applied Physics* 2008; **103**: 094515.